# Nonlinear O(3) sigma model in discrete complex analysis

# Masaru Kamata†, Masayoshi Sekiguchi‡ and Yuuki Tadokoro§

Natural Science Education, National Institute of Technology, Kisarazu College, 2-11-1 Kiyomidai-Hiqashi, Kisarazu, Chiba, 292-0041, Japan

E-mail:  $^\dagger$ kamata@kisarazu.ac.jp,  $^\ddagger$ masa@kisarazu.ac.jp,  $^\$$ tado@nebula.n.kisarazu.ac.jp

**Abstract.** We examine a discrete version of the two-dimensional nonlinear O(3)sigma model derived from discrete complex analysis. We adopt two lattices, one rectangular, the other polar. We define a discrete energy  $E(f)^{\text{disc.}}$  and a discrete area  $\mathcal{A}(f)^{\text{disc.}}$ , where the function f is related to a stereographic projection governed by a unit vector of the model. The discrete energy and area satisfy the inequality  $E(f)^{\text{disc.}} > |\mathcal{A}(f)^{\text{disc.}}|$ , which is saturated if and only if the function f is discrete (anti-)holomorphic. We show for the rectangular lattice that, except for a factor 2, the discrete energy and the area tend to the usual continuous energy E(f) and the area  $\mathcal{A}(f) = 4\pi N, \ N \in \pi_2(S^2)$  as the lattice spacings tend to zero. In the polar lattice, we section the plane by 2M lines passing through the origin into 2M equal sectors and place vertices radially in a geometric progression with a common ratio q. For this polar lattice, the Euler-Lagrange equation derived from the discrete energy  $E(f)^{\text{disc.}}$ yields rotationally symmetric (anti-)holomorphic solutions  $f(z) = Cz^{\pm 1}$  ( $C\bar{z}^{\pm 1}$ ) in the zeroth order of  $\kappa := q^{-1} - q$ . We find that the discrete area evaluated by these zerothorder solutions is expressible as a q-integral (the Jackson integral). Moreover, the area tends to  $\pm 2 \cdot 4\pi$  in the continuum limit  $(M \to \infty \text{ and } q \to 1-0)$  with fixed discrete conformal structure  $\rho_0 = 2\sin(\pi/M)/\kappa$ .

Keywords: nonlinear sigma model; discretization; discrete complex analysis; q-integral.

#### 1. Introduction

There exist prominent topological objects in a certain class of field theories. In four-dimensional Euclidean space  $\mathbb{R}^4$ , the BPST instanton [1] is a solution to the (anti-)self-dual Yang-Mills equations  $F_{\mu\nu} = \pm *F_{\mu\nu}$  that minimizes the action

$$S = \frac{1}{2} \text{Tr} \int_{\mathbb{R}^4} d^4 x \, F_{\mu\nu}^2 = \|F \mp *F\|^2 \pm 8\pi^2 N \ge 8\pi^2 |N|, \tag{1}$$

where  $\|\cdot\|$  is some norm and  $N \in \pi_3(S^3)$  is the instanton number. Similarly, the BPS monopole [2] in  $\mathbb{R}^3$  is a solution to the (anti-)Bogomol'nyi equations  $F_{jk} = \pm \varepsilon_{jkl} D_l \phi$ 

that minimizes the energy

$$E = \frac{1}{2} \operatorname{Tr} \int_{\mathbb{R}^3} d^3 x \left[ \mathbf{B}^2 + (\mathbf{D}\phi)^2 \right] = \|F \mp *D\phi\|^2 \pm 4\pi |\langle \phi \rangle| N \ge 4\pi |\langle \phi \rangle| |N|. \tag{2}$$

Here **B** is the magnetic field,  $\langle \phi \rangle$  the vacuum expectation value of the Higgs scalar  $\phi$ , and  $N \in \pi_2(S^2)$  a topological number that is proportional to the magnetic charge.

In  $\mathbb{R}^2$ , the nonlinear O(3) sigma model or the  $\mathbb{C}P^{N-1}$  model with  $\mathcal{N}=2$ , shares the above properties with instantons and monopoles. Indeed, we can show that the energy E of this model fulfils the following inequality

$$E = \frac{1}{2} \int_{\mathbb{R}^2} d^2 x \, (\partial_{\mu} n^j)^2 = \left\| \frac{df \mp i * df}{1 + |f|^2} \right\|^2 \pm 4\pi N \ge 4\pi |N|. \tag{3}$$

Here  $(n^j)_{j=1,2,3} =: \mathbf{n}(x,y)$  is a unit vector of  $\mathbb{R}^2 \cong \mathbb{C}$ . A function f of  $z = x + iy \in \mathbb{C}$  is defined by a stereographic projection from a sphere  $S^2_{|n|=1}$  to  $\mathbb{C}$  and its explicit form is given by [3, 4, 5]

$$f := \frac{n^1 + in^2}{1 + n^3}. (4)$$

The norm of a 1-form  $\alpha$  and the Hermitian scalar product of two 1-forms  $\alpha$  and  $\beta$  are defined by  $\|\alpha\|^2 = (\alpha, \alpha)$  and  $(\alpha, \beta) = \int_{\mathbb{R}^2} d^2x \, g^{\mu\nu}(x) \alpha_{\mu}(x) \bar{\beta}_{\nu}(x)$ , respectively; here the metric is set to  $g^{\mu\nu} = \text{diag}(1,1)$  for this paper. Note that we need appropriate boundary conditions on the vector  $\boldsymbol{n}$  at infinity to ensure the energy E of (3) finite. The topological number  $N \in \pi_2(S^2)$ , which classifies the map  $\boldsymbol{n}: S^2 \cong \mathbb{C} \cup \{\infty\} \to S^2_{|\boldsymbol{n}|=1}$ , is defined by

$$N = \frac{1}{4\pi} \int_{\mathbb{R}^2} d^2 x \, \boldsymbol{n} \cdot (\partial_x \boldsymbol{n} \times \partial_y \boldsymbol{n}). \tag{5}$$

If the complex function f(z) (4) is (anti-)holomorphic, then its real and imaginary parts satisfy the Cauchy–Riemann equations (or their anti-versions), which are expressible in a coordinate-independent manner as  $df \mp i * df = 0$ . Moreover, N is (negative) positive as seen immediately from the positive semi-definiteness of the energy E of (3). In these holomorphic and anti-holomorphic cases, we have the equality  $E = 4\pi |N|$ , and the (anti-)holomorphic function f gives a classical (anti-)instanton solution. The nonlinear O(3) sigma model is used in [3] to describe two-dimensional isotropic ferromagnetism and the general instanton solution with arbitrary  $N \in \mathbb{N}$  is obtained there.

The construction of discrete models on a lattice that maintains their topological stabilities is a challenging problem and was studied intensively a few decades ago: [6] for definition of a topological number, [7] for the sine-Gordon system with the Bogomol'nyi bound, [8, 9] for the Skyrme model, and [10, 11] for the O(3) sigma model. In particular, Ward [11] argues that, under certain general assumptions, the energy of any configuration with nonzero topological number of [6] is strictly greater than that of the Bogomol'nyi bound.

Meanwhile, the discrete complex analysis has a somewhat long history. There exist many concepts and theorems corresponding to those in ordinary complex analysis, such as the discrete holomorphic function, harmonic function, and Cauchy's integral theorem.

Wilson [12] used a triangular cellular decomposition of the Riemann surface and Mercat [13, 14] used arbitrary two-dimensional metric graphs and their dual graphs. They both obtained, for example, discrete period matrices, which in the continuum limit tend to the usual period matrix. Bobenko [15] developed a discrete differential geometry and applied it to the discrete integrable equations. Bobenko and Günther [16] presented a comprehensive theory of discrete Riemann surfaces in which medial graphs play some role. The introduction provides a more detailed description of the history.

The aim here is to reconstruct a discrete version of the nonlinear O(3) sigma model on lattices through a rather distinctive approach, specifically, through the discrete complex analysis of Mercat [13, 14]. In this theory, the discrete differential operator  $d_G$  or the coboundary operator dual to the boundary operator  $\partial$  acting on the graph G is defined for every two-dimensional graph G. Integrals of forms over the elements of G (vertices, edges and faces) are defined by Stokes' formulae. We adopt two graphs; a rectangular lattice and a polar lattice (or "spider-web" lattice). By expanding the norm squared  $\|(df \mp i * df)/(1 + |f|^2)\|^2$  in discrete quantities of the rectangular lattice, for example, we obtain a discrete energy  $E(f)_{(2a,2b)}^{\text{disc.}}$  (21), a discrete area  $\mathcal{A}(f)_{(2a,2b)}^{\text{disc.}}$  (22), and an inequality  $E(f)_{(2a,2b)}^{\text{disc.}} \geq |\mathcal{A}(f)_{(2a,2b)}^{\text{disc.}}|$  (20) relating the two. The inequality is saturated if and only if the function f is discrete (anti-)holomorphic; that is,  $df \mp i * df = 0$ . Except for a factor 2, the discrete energy and the area tend to the usual continuous energy E(f) and the area  $\mathcal{A}(f) = 4\pi N$ , respectively, as the lattice spacings tend to zero. The geometrical meaning of the area (22) is, however, unclear at present; it is especially not a priori a topological invariant. Our discrete energy (21), even though it fulfils the inequality (20), does not necessarily ensure topological stability of the solutions to the Euler-Lagrange equation stemmed from the discrete energy (21).

To investigate the topological aspects of the model, we introduce the polar lattice; we divide  $2\pi$  rotation about the origin into 2M equal sectors with some positive integer M and place the vertices radially in a geometric progression with a real common ratio q (0 < q < 1). The polar lattice is suitable in studying rotationally symmetric configurations such as the simplest non-trivial discrete (anti-)holomorphic function  $z = re^{i\theta}$  ( $\bar{z} = re^{-i\theta}$ ). The Euler-Lagrange equation derived from the discrete energy  $E(f)_{(M,q)}^{\text{disc.}}$  yields rotationally symmetric (anti-)holomorphic solutions  $f(z) = Cz^{\pm 1}$  ( $C\bar{z}^{\pm 1}$ ) in the zeroth order of the parameter  $\kappa := q^{-1} - q$ . We find that the discrete area  $\mathcal{A}(Cz^{\pm 1})_{(M,q)}^{\text{disc.}} = -\mathcal{A}(C\bar{z}^{\pm 1})_{(M,q)}^{\text{disc.}}$  evaluated using these zeroth-order solutions is expressible as a q-integral (or Jackson integral). Moreover, the area tends to the expected value  $\pm 2 \cdot 4\pi$  in the continuum limit for which  $M \to \infty$ ,  $q \to 1-0$ , and the discrete conformal structure  $\rho_0 = 2q \sin(\pi/M)/(1-q^2)$  (43) is fixed.

This paper is organized as follows. In Section 2, we adopt a two-dimensional rectangular graph  $\Gamma$ . In Section 2.1, we define a discrete version of the nonlinear O(3) sigma model on a double graph  $\Lambda := \Gamma \cup \Gamma^*$ , with  $\Gamma^*$  the dual graph to  $\Gamma$ . A discrete energy (21) and a discrete area (22) are defined, and we obtain an inequality (20) relating the two. In Section 2.2, we see that the discrete model tends to its continuum version, up to a factor 2, when the lattice spacings tend to zero. In Section 2.3, we derive the

Euler-Lagrange equation from the discrete energy (21) and the equation tends to the usual expression when the lattice spacings tend to zero. In Section 3, we adopt the polar lattice, first showing that the functions  $z^n$  with  $n=0, \pm 1$  are discrete holomorphic on the polar lattice, and second using the rotationally symmetric ansätze  $f(z) = h(r)e^{\pm i\theta}$  in the Euler-Lagrange equation to obtain a radial difference equation (56) for the unknown function h(r). By expanding the difference equation in the parameter  $\kappa$  we have a radial differential equation in the zeroth order of  $\kappa$  and obtain the (anti-)holomorphic solutions  $f(z) = Cz^{\pm 1} (C\bar{z}^{\pm 1})$  to this equation. Subsequently, we find that the discrete area  $\mathcal{A}(Cz^{\pm 1})_{(M,q)}^{\text{disc.}} = -\mathcal{A}(C\bar{z}^{\pm 1})_{(M,q)}^{\text{disc.}}$  evaluated by the zeroth-order solutions is expressible as the q-integral. This discrete area tends to  $\pm 2 \cdot 4\pi$ , as expected, in the continuum limit where the discrete conformal structure  $\rho_0$  (43) is fixed. Section 4 is devoted to conclusion and remarks.

#### 2. Discretization on a rectangular lattice

#### 2.1. Discrete energy and area defined on the lattice

We define [13, 14] the (oriented) double graph  $\Lambda := \Gamma \cup \Gamma^*$ , where  $\Gamma = \Gamma_0 \cup \Gamma_1 \cup \Gamma_2$  is a union of vertices  $\Gamma_0$ , edges  $\Gamma_1$ , and faces  $\Gamma_2$ , and  $\Gamma^*$  is the dual graph to  $\Gamma$ . Note that the edges are oriented and  $e^{**} = -e$  under successive operations of the dual. We define a discrete metric  $\ell$  on edges  $\Lambda_1 = \Gamma_1 \cup \Gamma_1^*$ , the value of which is the positive length of the edge  $e \in \Lambda_1$ . A discrete conformal structure  $\rho$  on edges  $\Lambda_1$  is a real positive function, its value being the ratio of the lengths  $\rho(e) := \ell(e^*)/\ell(e)$ . In the following, we adopt a simple rectangular graph  $\Gamma$  with lattice spacings (2a, 2b), where a and b are real positive constants (Fig. 1).

We have  $\rho(e) = b/a$  for any horizontal edge  $e \in \Gamma_1$  and  $\rho(e) = a/b$  for any vertical edge  $e \in \Gamma_1$ , with similar positive values for  $e \in \Gamma_1^*$ .

To derive a discrete expression for the nonlinear O(3) sigma model, we now expand the norm squared  $\|(df \mp i * df)/(1 + |f|^2)\|^2$  using discrete quantities defined on  $\Lambda$ . Here d and \* are, respectively, the discrete differential operator and the Hodge star operator on forms; they are defined in the following way.

For every two-dimensional graph G, we define a discrete differential operator  $d_G$  or a coboundary operator dual to the boundary operator  $\partial$  acting on the graph G. The application of  $d_{\Lambda} =: d$  to 0- and 1-forms is defined [13, 14] as follows

$$\int_{e} df := f(e_{+}) - f(e_{-}), \tag{6}$$

$$\iint_{F} d\alpha := \oint_{\partial F} \alpha,\tag{7}$$

where  $f \in C^0(\Lambda)$  is a 0-form, i.e., an ordinary function,  $\alpha \in C^1(\Lambda)$  is a 1-form, and  $e_+$  and  $e_-$  denote the terminal and initial points of the edge e, respectively. Definitions (6) and (7) can be considered as Stokes' formulae. The Hodge star operator \* on the

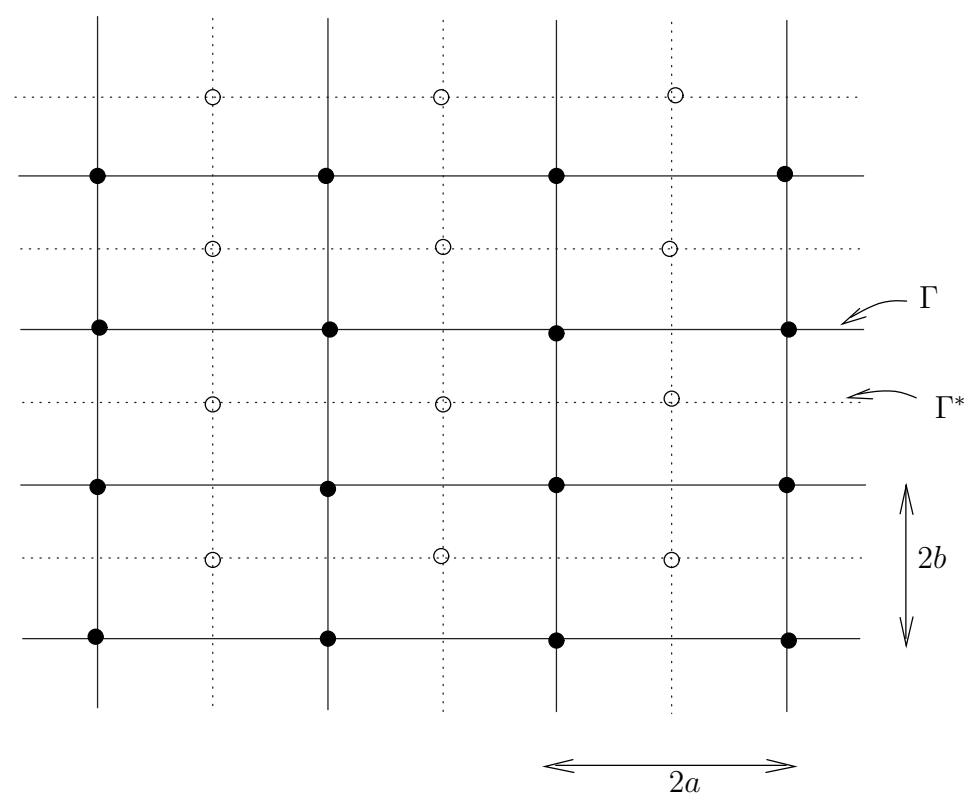


Figure 1. Two-dimensional graph  $\Lambda = \Gamma \cup \Gamma^*$ , Solid line —— :  $\Gamma$ , Dotted line · · · · · :  $\Gamma^*$ 

1-form  $\alpha$  is defined through the dual graph  $\Gamma^*$  by

$$\int_{e} *\alpha := -\rho(e^*) \int_{e^*} \alpha, \tag{8}$$

with similar definitions for 0- and 2-forms, although we do not use them in this paper. A function f is said to be discrete (anti-)holomorphic if it satisfies the discrete Cauchy–Riemann equations (or their anti-versions)

$$df \mp i * df = 0. (9)$$

If we integrate both sides of (9) along any edge  $e \in \Lambda_1$ , then the formulae (6) and (8) induce the equation

$$f(e_{+}) - f(e_{-}) \pm i\rho(e^{*}) \left( f(e_{+}^{*}) - f(e_{-}^{*}) \right) = 0, \tag{10}$$

which is a finite version of the discrete Cauchy–Riemann equations (or their antiversions) (9).

To proceed further, we need, in accordance with an argument of [13, 14], the following definition

$$\int_{e} f \cdot \alpha := \frac{f(e_{+}) + f(e_{-})}{2} \int_{e} \alpha. \tag{11}$$

This ensures that the operator d is a derivation for functions f and g, i.e., it obeys the Leibniz rule for their product:

$$d(fg) = g df + f dg. (12)$$

If we integrate both sides of (12) along an arbitrary edge  $e \in \Lambda_1$ , then we have from (6) and (11) the identity

$$f(e_{+})g(e_{+}) - f(e_{-})g(e_{-}) = \frac{g(e_{+}) + g(e_{-})}{2}(f(e_{+}) - f(e_{-})) + \{f \leftrightarrow g\}, \tag{13}$$

where  $\{f \leftrightarrow g\}$  denotes the term obtained from the preceding term by interchanging f and g. Conversely, if we start with the identity (13), then we obtain (12) through (11) as the edge  $e \in \Lambda_1$  is arbitrary. We say that the infinitesimal relation (12) and the finite version (13) are equivalent. We then have

$$\int_{e} \frac{df \mp i * df}{1 + |f|^2} = \frac{\lambda(e_+) + \lambda(e_-)}{2} \Big( f(e_+) - f(e_-) \pm i\rho(e^*) (f(e_+^*) - f(e_-^*)) \Big), \tag{14}$$

where  $\lambda(z)$  is defined by

$$\lambda(z) := \frac{1}{1 + |f(z)|^2} = \frac{1 + n^3(z)}{2}.$$
 (15)

A discrete norm of a 1-form  $\alpha$  is defined by  $\|\alpha\|^2 := (\alpha, \alpha)$  as usual, and a discrete Hermitian scalar product of two 1-forms  $\alpha$  and  $\beta$  is defined using the discrete quantities on the edges  $\Lambda_1$  [13, 14],

$$(\alpha, \beta) = \sum_{e \in \Lambda_1} \rho(e) \left( \int_e \alpha \right) \left( \int_e \bar{\beta} \right), \tag{16}$$

where the edge e runs over the infinite number of edges  $\Lambda_1$ . From (14) and (16), we have

$$\left\| \frac{df \mp i * df}{1 + |f|^2} \right\|^2$$

$$= \sum_{e \in \Gamma_1} \nu(e_+, e_-, e_+^*, e_-^*) \left| \sqrt{\rho(e)} (f(e_+) - f(e_-)) \pm i \sqrt{\rho(e^*)} (f(e_+^*) - f(e_-^*)) \right|^2 \ge 0. \quad (17)$$

Here,

$$\nu(e_+, e_-, e_+^*, e_-^*) := \left(\frac{\lambda(e_+) + \lambda(e_-)}{2}\right)^2 + \{e \to e^*\},\tag{18}$$

in which  $\{e \to e^*\}$  denotes the term obtained from the preceding term by replacing e with  $e^*$ . In the derivation of (17), we used the formula

$$\sum_{e \in \Lambda_1} F(e) = \sum_{e \in \Gamma_1} \Big( F(e) + F(e^*) \Big), \tag{19}$$

which holds for any function F of e because  $\Lambda_1 = \Gamma_1 \cup \Gamma_1^*$ . From (17), we immediately obtain a discrete version of the inequality (3)

$$E_{(2a,2b)}^{\text{disc.}} = \left\| \frac{df \mp i * df}{1 + |f|^2} \right\|^2 \pm \mathcal{A}(f)_{(2a,2b)}^{\text{disc.}} \ge |\mathcal{A}(f)_{(2a,2b)}^{\text{disc.}}|, \tag{20}$$

where the discrete energy and area are defined by

$$E_{(2a,2b)}^{\text{disc.}} := \sum_{e \in \Gamma_1} \nu(e_+, e_-, e_+^*, e_-^*) \Big( \rho(e) |f(e_+) - f(e_-)|^2 + \{e \to e^*\} \Big) \ge 0, \quad (21)$$

$$\mathcal{A}(f)_{(2a,2b)}^{\text{disc.}} := -2 \operatorname{Im} \sum_{e \in \Gamma_{1}} \nu(e_{+}, e_{-}, e_{+}^{*}, e_{-}^{*}) \left( f(e_{+}) - f(e_{-}) \right) \left( \overline{f(e_{+}^{*}) - f(e_{-}^{*})} \right). \tag{22}$$

Here the dependence on the lattice spacings 2a and 2b is explicitly denoted by a subscript. Note that the discrete energy (21) is positive semi-definite and depends on the discrete conformal structure  $\rho$ , whereas the discrete area (22) does not have these properties. To express (21) and (22) in terms of the vector  $\boldsymbol{n}$ , we use the following relations

$$|f(e_{+}) - f(e_{-})|^{2} = \frac{1}{4\lambda(e_{+})\lambda(e_{-})}|\boldsymbol{n}(e_{+}) - \boldsymbol{n}(e_{-})|^{2},$$
(23)

$$\operatorname{Im}\{(f(e_{+}) - f(e_{-}))(\overline{f(e_{+}^{*}) - f(e_{-}^{*})})\}$$

$$= -\frac{1}{4} \left\{ \left( \frac{\boldsymbol{n}(e_{+})}{\lambda(e_{+})} - \frac{\boldsymbol{n}(e_{-})}{\lambda(e_{-})} \right) \times \left( \frac{\boldsymbol{n}(e_{+}^{*})}{\lambda(e_{+}^{*})} - \frac{\boldsymbol{n}(e_{-}^{*})}{\lambda(e_{-}^{*})} \right) \right\}^{3}.$$
(24)

These are direct consequences of the definition (4) of the function f. The symbol  $\{\cdots\}^3$  in (24) stands for the third component of the vector in the curly brackets. Substituting (23) and (24) into (21) and (22), respectively, we obtain the following discrete energy and area expressed in the vector  $\mathbf{n}$ 

$$E_{(2a,2b)}^{\text{disc.}} = \frac{1}{4} \sum_{e \in \Gamma_1} \nu(e_+, e_-, e_+^*, e_-^*) \left( \frac{\rho(e)}{\lambda(e_+)\lambda(e_-)} |\boldsymbol{n}(e_+) - \boldsymbol{n}(e_-)|^2 + \{e \to e^*\} \right), \quad (25)$$

$$\mathcal{A}(f)_{(2a,2b)}^{\text{disc.}} = \frac{1}{2} \sum_{e \in \Gamma_1} \nu(e_+, e_-, e_+^*, e_-^*) \left\{ \left( \frac{\boldsymbol{n}(e_+)}{\lambda(e_+)} - \frac{\boldsymbol{n}(e_-)}{\lambda(e_-)} \right) \times \left( \frac{\boldsymbol{n}(e_+^*)}{\lambda(e_+^*)} - \frac{\boldsymbol{n}(e_-^*)}{\lambda(e_-^*)} \right) \right\}^3. (26)$$

Note that the discrete energy (25) is positive semi-definite and invariant under the interchange  $\mathbf{n}(e_+) \leftrightarrow \mathbf{n}(e_-)$  and/or the interchange  $\mathbf{n}(e_+^*) \leftrightarrow \mathbf{n}(e_-^*)$ , whereas the discrete area (26) does not have these properties. Moreover, the discrete energy (25) includes the Hamiltonian of the Heisenberg model  $\mathcal{H}_{\text{Heisenberg}} = -\sum_{i,j} J_{ij} \mathbf{S}_i \cdot \mathbf{S}_j$ , where  $\mathbf{S} = \mathbf{n}$ , and indices i and j run over nearest-neighbour lattice sites; here the coupling  $J_{ij}$  is, however, not constant and field-dependent.

## 2.2. Continuum limit of the discrete energy and the area

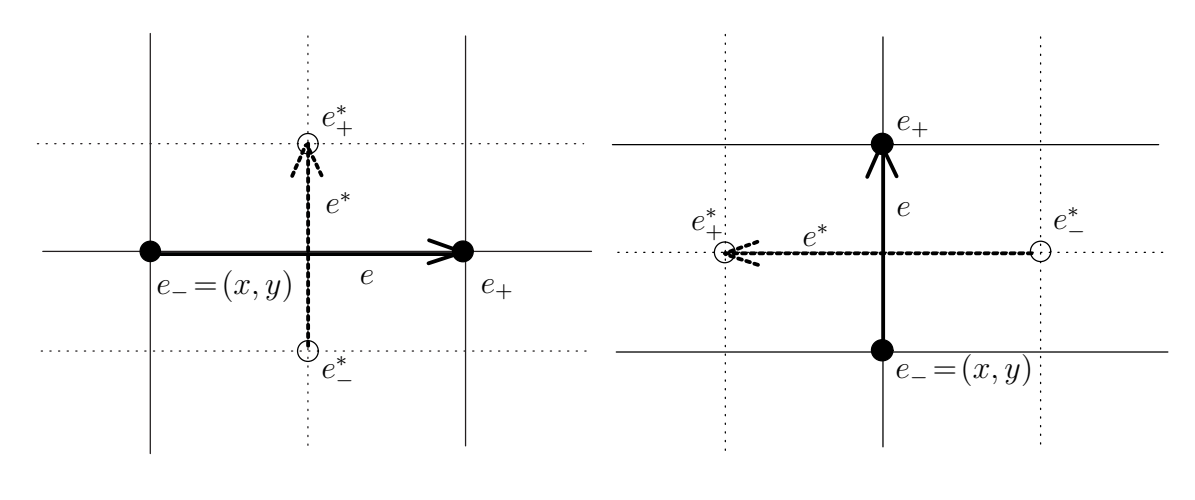
We now consider the continuum limit of the discrete nonlinear O(3) sigma model in the preceding section. As the lattice spacings (2a, 2b) tend to (+0, +0), we have, for the horizontal edge  $e \in \Gamma_1$ , the following limit

$$\rho(e)|\mathbf{n}(e_{+}) - \mathbf{n}(e_{-})|^{2} = \frac{b}{a} \cdot 4a^{2} \left| \frac{\mathbf{n}(e_{+}) - \mathbf{n}(e_{-})}{2a} \right|^{2}$$

$$= \Delta x \Delta y \left| \frac{\mathbf{n}(x + \Delta x, y) - \mathbf{n}(x, y)}{\Delta x} \right|^{2}$$

$$\to dx dy \left| \frac{\partial \mathbf{n}(x, y)}{\partial x} \right|^{2}, \tag{27}$$

where  $\Delta x := 2a$ ,  $\Delta y := 2b$ , and the initial point of e is here denoted by (x, y), i.e.,  $(x, y) := e_-$  (Fig. 2).



e: horizontal e: vertical

**Figure 2.** Edge e and its dual edge  $e^*$ 

Similarly, for vertical edge  $e \in \Gamma_1$ , we have

$$\rho(e)|\boldsymbol{n}(e_{+}) - \boldsymbol{n}(e_{-})|^{2} \to dxdy \left| \frac{\partial \boldsymbol{n}(x,y)}{\partial y} \right|^{2}. \tag{28}$$

We proceed further to the vertical edge  $e^*$ , which is dual to the horizontal edge  $e \in \Gamma_1$ , and we have

$$\rho(e^*)|\boldsymbol{n}(e_+^*) - \boldsymbol{n}(e_-^*)|^2 = \Delta x \Delta y \left| \frac{\boldsymbol{n}(x + \Delta x/2, y + \Delta y/2) - \boldsymbol{n}(x + \Delta x/2, y - \Delta y/2)}{\Delta y} \right|^2$$

$$\to dxdy \left| \frac{\partial \boldsymbol{n}(x, y)}{\partial y} \right|^2. \tag{29}$$

For the horizontal edge  $e^*$ , which is dual to vertical edge  $e \in \Gamma_1$ , we have

$$\rho(e^*)|\boldsymbol{n}(e_+^*) - \boldsymbol{n}(e_-^*)|^2 \to dxdy \left| \frac{\partial \boldsymbol{n}(x,y)}{\partial x} \right|^2.$$
(30)

Summing up the above terms, we have the following continuum limit of the discrete energy (25)

$$E_{(2a,2b)}^{\text{disc.}} \to \frac{1}{4} \int_{\mathbb{P}^2} d^2 x \ 2\Big(2|\partial_x \boldsymbol{n}|^2 + 2|\partial_y \boldsymbol{n}|^2\Big) = \int_{\mathbb{P}^2} d^2 x (\partial_\mu n^\alpha)^2 = 2E,$$
 (31)

where  $d^2x := dxdy$  and we have used the fact that

$$\lambda(e_+) \to \lambda(e_-), \quad \nu(e_+, e_-, e_+^*, e_-^*) \to 2\lambda^2(e_-).$$
 (32)

To obtain the continuum limit of the discrete area, we first note the limit

$$\left(\frac{\boldsymbol{n}(e_{+})}{\lambda(e_{+})} - \frac{\boldsymbol{n}(e_{-})}{\lambda(e_{-})}\right) \times \left(\frac{\boldsymbol{n}(e_{+}^{*})}{\lambda(e_{+}^{*})} - \frac{\boldsymbol{n}(e_{-}^{*})}{\lambda(e_{-}^{*})}\right) 
\rightarrow dxdy \,\partial_{x}\left(\frac{\boldsymbol{n}}{\lambda}\right) \times \partial_{y}\left(\frac{\boldsymbol{n}}{\lambda}\right) = dxdy \frac{1}{2\lambda^{3}}(n^{1}, n^{2}, n^{3} + 1) \,\boldsymbol{n} \cdot (\partial_{x}\boldsymbol{n} \times \partial_{y}\boldsymbol{n}), \tag{33}$$

where the arguments of  $\mathbf{n}$  and  $\lambda$  in (33) are (x, y) and the vector product  $\partial_x \mathbf{n} \times \partial_y \mathbf{n}$  is proportional to the vector  $\mathbf{n}$ . Equations (26) and (33) give

$$\mathcal{A}(f)_{(2a,2b)}^{\text{disc.}} \to \frac{1}{2} \int_{\mathbb{R}^2} d^2 x \, 2 \cdot 2 \, \boldsymbol{n} \cdot (\partial_x \boldsymbol{n} \times \partial_y \boldsymbol{n}) = 2 \cdot 4\pi N. \tag{34}$$

The factor 2 in front of E of (31) and  $4\pi N$  of (34) requires explanation. Because the faces of the two graphs  $\Gamma$  and  $\Gamma^*$  overlap and, in a sense, the continuum limit of both graphs is the two-dimensional continuous space  $\mathbb{R}^2$ , the continuum limit of the double graph  $\Lambda = \Gamma \cup \Gamma^*$  can be expressed as  $2\mathbb{R}^2$ . If this argument for the limit of the double graph  $\Lambda$  is legitimate, then it enables us to rewrite (31) and (34) as integrals over  $2\mathbb{R}^2$ ,

$$E_{(2a,2b)}^{\text{disc.}} \rightarrow \int_{\mathbb{R}^2} d^2 x (\partial_{\mu} n^{\alpha})^2 = \frac{1}{2} \int_{2\mathbb{R}^2} d^2 x (\partial_{\mu} n^{\alpha})^2,$$
 (35)

$$\mathcal{A}(f)_{(2a,2b)}^{\text{disc.}} \to 2 \cdot \int_{\mathbb{R}^2} d^2 x \ \boldsymbol{n} \cdot (\partial_x \boldsymbol{n} \times \partial_y \boldsymbol{n}) = \int_{2\mathbb{R}^2} d^2 x \ \boldsymbol{n} \cdot (\partial_x \boldsymbol{n} \times \partial_y \boldsymbol{n}), \tag{36}$$

with correct coefficients. While this explanation for the appearance of the factor 2 is rather intuitive, a more rigorous argument is possible. Note that this doubling may be inevitable in Mercat's discrete theory of complex analysis [13, 14], which is based on the double graph  $\Lambda = \Gamma \cup \Gamma^*$ .

Note that the discrete area (22) or (26) is an infinite double series over  $\mathbb{Z}^2$  and therefore its evaluation is not easy for general a and b. In contrast, the continuous area (5) can be easily evaluated by integrating the double integrals (see Appendix A).

# 2.3. The Euler-Lagrange equation and its continuum limit

Imposing the stationary condition  $\delta E_{(2a,2b)}^{\text{disc.}} = 0$  on the discrete energy (21), we obtain from the standard variational calculation the resulting Euler–Lagrange equation

$$[EL]^{\text{disc.}}(z) := \sum_{x \in Star(z)} \nu(x, z, e_+^*, e_-^*) \rho(x, z) (f(x) - f(z))$$

$$+ \frac{f(z)}{2(1+|f(z)|^2)^2} \sum_{x \in \text{Star}(z)} (\lambda(x) + \lambda(z)) \left( \rho(x,z)|f(x) - f(z)|^2 + \{e \to e^*\} \right) = 0, (37)$$

where  $\operatorname{Star}(z)$  is the set of nearest-neighbour points of z, and e is the edge from z to x. Note that the first sum in (37) is a weighted Laplacian with the weight  $\nu(x,z,e_+^*,e_-^*)\rho(x,z)$  and the second sum is derived from the variation of the weight. If the function f is discrete holomorphic, then the term  $\{e \to e^*\}$  in (37) is equal to the preceding term  $\rho(x,z)|f(x)-f(z)|^2$  and simplifies the expression.

As  $(2a, 2b) \rightarrow (+0, +0)$ , we obtain the following continuum limit

$$[EL]^{\text{disc.}} \to 2 \cdot 4ab[EL]^{\text{cont.}},$$
 (38)

where  $4ab = 2a \times 2b$  is the area of the smallest rectangle of  $\Gamma$  or  $\Gamma^*$ , and [EL]<sup>cont.</sup> is defined by

$$[EL]^{\text{cont.}} := \partial_{\mu} \left( \frac{\partial^{\mu} f}{(1+|f|^{2})^{2}} \right) + \frac{2f}{(1+|f|^{2})^{3}} |\partial_{\mu} f|^{2}$$
(39)

$$= \frac{4}{(1+|f|^2)^2} \left( \partial_z \partial_{\bar{z}} f - \frac{2\bar{f}}{1+|f|^2} \partial_z f \cdot \partial_{\bar{z}} f \right). \tag{40}$$

In deriving (40), we have used the relation  $\partial_{\mu}\partial^{\mu} = \Delta = 4\partial_{z}\partial_{\bar{z}}$ . Expression (40) manifests the fact that holomorphic functions ( $\partial_{\bar{z}}f = 0$ ) or anti-holomorphic functions ( $\partial_{z}f = 0$ ) solve the continuum Euler-Lagrange equation [EL]<sup>cont.</sup> = 0.

In general, the linear function is discrete holomorphic for any graph and the quadratic function is discrete holomorphic only for parallelogram graphs. In Appendix A, we illustrate briefly several continuum instanton solutions obtained from these linear and quadratic functions.

In the next section, we introduce the polar lattice, which is more suitable than the rectangular lattice in studying rotationally symmetric configurations such as the (discrete) holomorphic function  $z = re^{i\theta}$  or anti-holomorphic function  $\bar{z} = re^{-i\theta}$ .

#### 3. Discretization on the polar lattice

## 3.1. Polar lattice and the discrete (anti-)holomorphic functions

Here we introduce the polar lattice and consider discrete (anti-) holomorphic functions on it. In our polar lattice, the polar coordinates  $(r, \theta)$  of the vertices  $\Lambda_0 = \Gamma_0 \cup \Gamma_0^*$  are restricted to certain "even" and "odd" values according to the rule

$$(r,\theta) = \begin{cases} (aq^{2k}, 2l\alpha) & \text{for } z \in \Gamma_0, \\ (aq^{2k+1}, (2l+1)\alpha) & \text{for } z \in \Gamma_0^*, \end{cases}$$

$$(41)$$

where  $k \in \mathbb{Z}$  and  $l = 0, 1, 2, \dots, M - 1$  with some positive integer M. We divide the plane into 2M equal sectors centred about the origin, each sector having included angle  $\alpha := 2\pi/(2M) = \pi/M$ . We assume all edges are straight-line segments. Figure 3

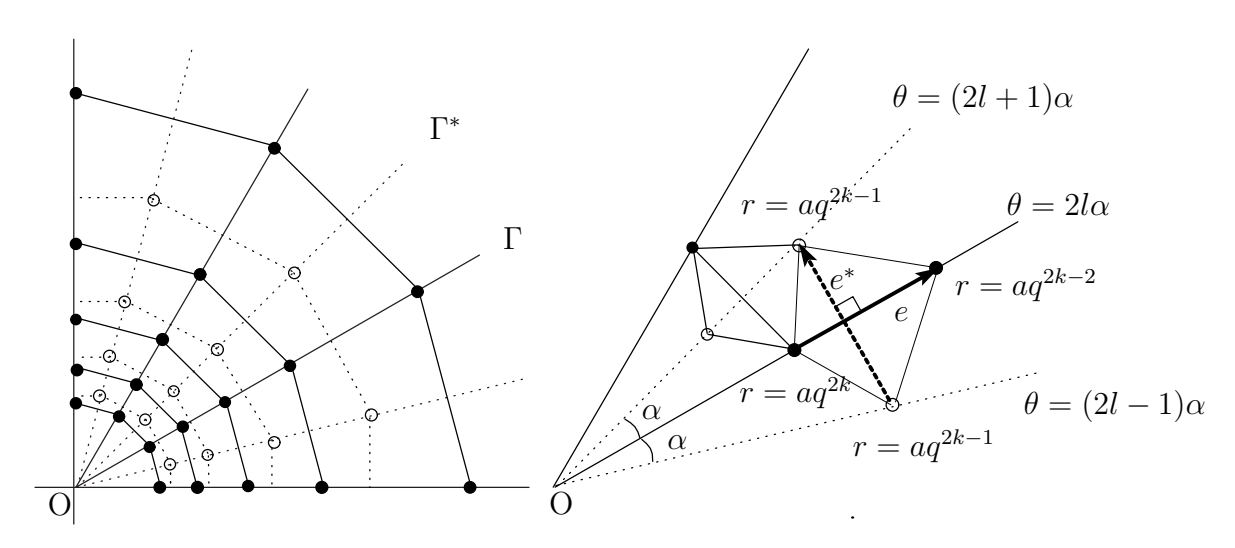


Figure 3. A polar ("spider-web") lattice with M=12 and two neighbouring kites

depicts the first quadrant of a polar lattice with M=12. Parameters a and q are real constants with a>0 and 0< q<1. We call the vertices of  $\Gamma$  and  $\Gamma^*$  even and odd vertices, respectively, which for our bipartite graph also correspond to the black

and white vertices. Note that the radii of the vertices form a geometric progression with initial length a and common ratio q. Moreover, the origin and infinity are its accumulation points.

An edge e and its dual  $e^*$  of the polar lattice form a kite and these two edges are orthogonal to each other. All the kites are similar to each other. Indeed, the vertices of the small kite of Fig. 3 are obtained from those of the large kite by multiplying by  $qe^{i\alpha}$ , which induces a scaling by scale factor q and a rotation by angle  $\alpha$  of the large kite. In particular, the similarity ratio of two neighbouring kites with a common edge such as those in Fig. 3 is q. The area  $S_n$  of the kite with the radial diagonal ranging from  $r = aq^n$  to  $r = aq^{n-2}$  is given by

$$S_n = a^2 q^{2n-3} (1 - q^2) \sin \alpha. \tag{42}$$

Moreover, the discrete conformal structure  $\rho(e) = \ell(e^*)/\ell(e)$  of the radial edge e of the large kite in Fig. 3 is given by

$$\rho(e) = \frac{2q \sin \alpha}{1 - q^2} =: \rho_0, \tag{43}$$

which depends only on the parameters  $\alpha = \pi/M$  and q but not on k, a consequence of the similarity of all the kites. In Section 3.3, we shall consider a continuum limit where  $\alpha \to +0$  and  $q \to 1-0$  with fixed discrete conformal structure (43). In the following, we also denote this fixed value by  $\rho_0$ .

Note that the function  $z^{-1}$ , which is not discrete holomorphic on the rectangular lattice (Section 2), is discrete holomorphic on the polar lattice, as can be easily seen by verifying the definition (10). Therefore, we find discrete holomorphic functions  $z^n$ ,  $n = 0, \pm 1$  on the polar lattice. In addition to these functions, we have the dual discrete holomorphic functions  $(z^n)^{\dagger}$ . Here dagger denotes the dual [17, 18]; the dual of a discrete holomorphic function f is defined by

$$f^{\dagger}(z) := \varepsilon(z)\bar{f}(z),$$
 (44)

in which  $\varepsilon$  is the bi-constant satisfying  $\varepsilon|_{\Gamma} = +1$  and  $\varepsilon|_{\Gamma^*} = -1$  and  $\bar{f}$  denotes the complex conjugation of f. Including the dual, we have the following discrete holomorphic function

$$f(z) = \sum_{n=0, \pm 1} \left( C_n z^n + \tilde{C}_n(z^n)^{\dagger} \right), \tag{45}$$

with constants  $C_n$  and  $\tilde{C}_n$ . Note that  $1^{\dagger} = \varepsilon(z)$ . We consider (45) as a Laurent series expansion of the discrete holomorphic function f(z).

Depending on their angular behaviour about the origin, the linear combination (45) divides into three parts

$$C_0 + \tilde{C}_0 1^{\dagger}, \ C_1 z + \tilde{C}_{-1} (z^{-1})^{\dagger}, \ C_{-1} z^{-1} + \tilde{C}_1 z^{\dagger},$$
 (46)

or more explicitly by substituting  $z = re^{i\theta}$ 

$$C_0 + \tilde{C}_0 \epsilon(r), \left( C_1 r + \tilde{C}_{-1} \epsilon(r) r^{-1} \right) e^{i\theta}, \left( C_{-1} r^{-1} + \tilde{C}_1 \epsilon(r) r \right) e^{-i\theta}, \tag{47}$$

where  $r = aq^n \ (n \in \mathbb{Z}), \ \theta = m\alpha \ (m = 0, 1, 2, \dots, 2M - 1)$  and  $\epsilon(r)$  is defined by

$$\epsilon(r) = \epsilon(aq^n) := (-1)^n. \tag{48}$$

To study the radial behaviour of the function f(z), we here introduce the shift operator S,

$$Sf(z) := f(qe^{i\alpha}z). \tag{49}$$

Note that the bi-constant  $\varepsilon$  changes its sign under the shift operator S

$$S^{\pm 1}\varepsilon(z) = -\varepsilon(z),\tag{50}$$

because the operators  $S^{\pm 1}$  map specifically a vertex in  $\Gamma$  to one in  $\Gamma^*$ , and vice versa. Denoting the three linear combinations of (46) by  $f_0(z)$ ,  $f_+(z)$  and  $f_-(z)$ , respectively, we find that they obey the following relations

$$(S^{-1} - S)f_0(z) = 0, \quad (e^{\pm i\alpha}S^{-1} - e^{\mp i\alpha}S)f_{\pm}(z) = \pm \kappa f_{\pm}(z), \tag{51}$$

with corresponding sign choices, and  $\kappa$  is defined by

$$\kappa := q^{-1} - q = (1 - q^2)/q. \tag{52}$$

Putting  $f_{\pm}(z) = h_{\pm}(r)e^{\pm i\theta}$  in the second equations of (51), we have the following radial difference equations

$$h(q^{-1}r) - h(qr) = \pm \kappa h(r). \tag{53}$$

Because the bi-constant does not tend to any definite value as  $q \to 1-0$ , we need conditions  $\tilde{C}_n \to 0$   $(q \to 1-0)$  so that the function (45) has a limit. Under these conditions, the difference equations (53) yield differential equations

$$rh'(r) = \pm h(r), \tag{54}$$

for which the general solutions are  $h(r) = Cr^{\pm 1}$ . In other words, a discrete version of the differential equations (54) is the difference equations (53) that admit the bi-constant factors in its solutions. The function  $f(z) = z^{-1}$  yields the N = 1 instanton solution with the boundary conditions opposite to those of f(z) = z; see Appendix A for more detail.

Other discrete holomorphic functions such as the discrete exponential [13, 14] yield other type of difference equations. We do not discuss them in this paper.

#### 3.2. Rotationally symmetric ansätze and solutions to the Euler-Lagrange equation

Here we study the Euler–Lagrange equation (37), which can also be used in regard to the polar lattice, provided that vertices, edges, and faces are appropriately identified with those of the polar lattice. Hereafter, we use the following rotationally symmetric ansätze

$$f(z) = h(r)e^{\pm i\theta} \tag{55}$$

in the Euler-Lagrange equation (37), where h(r) is an unknown function of r. Moreover, in the following we assume a = 1 for the initial value a. This is equivalent to locating

M even vertices  $(r,\theta)=(aq^{2k},2l\alpha)=(1,2l\alpha)$  with k=0 and  $l=0,1,2,\cdots,M-1$  on the equator of the sphere  $S^2_{|n|=1}$ , with the centre assumed to be located at the coordinate origin. Vertices on  $\mathbb{R}^2\cong\mathbb{C}$  with k>0 and k<0 correspond to the points on the upper and lower hemispheres of  $S^2_{|n|=1}$ , respectively, through the stereographic projection. These points on the sphere are symmetric with respect to the complex plane  $\mathbb{C}$ .

Substituting the ansätze (55) into the Euler–Lagrange equation (37), we obtain the following difference equation for the function h(r)

$$[EL]^{\text{disc.}}(z)/(2e^{\pm i2l\alpha}q^{2}S_{0})$$

$$= \kappa^{-2}\nu(q^{-1}r)\left[h(q^{-2}r) - h(r)\right] + \kappa^{-2}\nu(qr)\left[h(q^{2}r) - h(r)\right] - \nu(r)h(r)$$

$$+ \frac{1}{2}\left\{\left[\lambda(q^{-2}r) + \lambda(r)\right]\left[\kappa^{-2}|h(q^{-2}r) - h(r)|^{2} + |h(q^{-1}r)|^{2}\right]\right.$$

$$+ \left[\lambda(q^{2}r) + \lambda(r)\right]\left[\kappa^{-2}|h(q^{2}r) - h(r)|^{2} + |h(qr)|^{2}\right]$$

$$+ 4\lambda(r)\left[\kappa^{-2}|h(qr) - h(q^{-1}r)|^{2} + |h(r)|^{2}\right]\lambda^{2}(r)h(r) = 0,$$
(56)

where we used  $Star(z) = \{q^2z, q^{-2}z, e^{i2\alpha}z, e^{-i2\alpha}z\}$  and defined

$$\nu(r) := \frac{1}{4} \left( \lambda(q^{-1}r) + \lambda(qr) \right)^2 + \lambda^2(r), \qquad \lambda(r) := \frac{1}{1 + |h(r)|^2}. \tag{57}$$

Note that the function  $\nu(r)$  of (57) is a shifted "four-point" function (18) evaluated by the edges e and  $e^*$  of Fig. 3, where  $e_+=q^{-2}z$ ,  $e_-=z$ ,  $e_+^*=q^{-1}e^{i\alpha}z$  and  $e_-^*=q^{-1}e^{-i\alpha}z$ ; specifically, we have

$$\nu(q^{-2}z, z, q^{-1}e^{i\alpha}z, q^{-1}e^{-i\alpha}z) = \frac{1}{4} \left(\lambda(q^{-2}r) + \lambda(r)\right)^2 + \lambda^2(q^{-1}r) = \nu(q^{-1}r).$$
 (58)

Because of the rotational symmetry of the ansätze (55) an overall factor  $e^{\pm i2l\alpha}$  appears in the Euler-Lagrange equation (37). Normalizing both sides of (37) by this factor, we obtain (56), which does not depend on the angular index l. Furthermore, we have normalized both sides of (56) by a typical value for the area of the kite  $S_0 = q^{-2}\kappa \sin \alpha$ .

The two-dimensional  $(r, \theta)$  difference equation (37) is reduced to the onedimensional (r) difference equation (56). Because (56) is highly nonlinear, it is not easy to obtain its exact solutions for generic values of q. In this paper we content ourselves with approximate solutions obtained in some continuum limit. If we take the limits where  $\alpha$  is fixed and  $q \to 1-0$ , or  $\alpha \to +0$  and q is fixed, then we have an infinite or a vanishing discrete conformal structure  $\rho_0 = 2 \sin \alpha / \kappa$  (43). This violates Zlámal's condition [19] known in the finite element method. In the following, we take a continuum limit where  $\alpha \to +0$  and  $q \to 1-0$  with fixed discrete conformal structure  $\rho_0$  (43).

In view of (56), we expand it in the parameter  $\kappa$  instead of q. Using formulae given in Appendix B, the difference equation (56) gives, in the zeroth order of  $\kappa$ , the following second-order differential equation for h(r)

$$r(r\lambda^2 h')' - \lambda^2 h + 2(r^2 |h'|^2 + |h|^2)\lambda^3 h = 0,$$
(59)

where  $\lambda$  is related to h through (57). By direct substitution, we immediately verify that the functions  $h(r) = Cr^{\pm 1}$  fulfil (59) with C being an arbitrary complex constant.

Conversely, we find that the differential equation (59) yields the solutions  $h(r) = Cr^{\pm 1}$ , provided that an appropriate boundary condition is imposed. To show this, we write with complete generality

$$h(r) = R(r)e^{i\phi(r)},\tag{60}$$

where R(r) and  $\phi(r)$  are real unknown functions of r. Note that the function h(r) introduced in the ansätze (55) is not assumed to be real; indeed we assume a complex h(r) below. Substituting (60) into the differential equation (59), its imaginary part gives, after an integration,

$$r\lambda^2 R^2 \phi' = c_1,\tag{61}$$

where  $c_1$  is a real constant of integration. Furthermore, the real part of (59) gives, after an integration,

$$r^{2} \left(\frac{dR}{dr}\right)^{2} = R^{2} - c_{1}^{2} R^{-2} (1 + R^{2})^{2} (1 + R^{4}) + c_{2} (1 + R^{2})^{2}, \tag{62}$$

with  $c_2$  a real constant of integration. Note that the equation (62) is, in a sense, invariant under the interchange  $R \leftrightarrow R^{-1}$ , i.e., if  $R_1$  is a solution to (62), then  $R_2 = R_1^{-1}$  is also a solution, being compatible with the projective nature of our  $\mathbb{C}P^1$  model. Now we impose the boundary condition

$$R(r) \to 0, \quad (r \to 0 \text{ or } \infty)$$
 (63)

on the function R(r). Comparing both sides of (62) under the boundary condition (63), we find  $c_1 = 0$  and  $c_2 \ge 0$ . Hence the differential equation (61) implies  $\phi = c_3$ , where  $c_3$  is a real constant of integration. Suppose  $c_2 > 0$ , then the differential equation (62) becomes, under the boundary condition (63),

$$r^2 \left(\frac{dR}{dr}\right)^2 = c_2 + o(R). \tag{64}$$

The asymptotic solutions to (64) are given by  $R = \pm \sqrt{c_2} \ln(r/r_0)$  with a positive constant  $r_0$ , but they do not fulfil the boundary condition (63); therefore, we find  $c_2 = 0$ . Solving  $r^2 \left(\frac{dR}{dr}\right)^2 = R^2$ , we have  $R = c_4 r^{\pm 1}$  with a real constant  $c_4$ , and finally we obtain  $h(r) = Cr^{\pm 1}$  through (60) with  $C := c_4 e^{ic_3}$ .

The functions  $h(r) = Cr^{\pm 1}$  and ansätze (55) yield the four solutions  $f(z) = Cz^{\pm 1}$  and  $f(z) = C\bar{z}^{\pm 1}$  to the difference equation (56) in the zeroth order of  $\kappa$ . These solutions are expected given the rotationally symmetric ansätze (55), because they correspond to the simplest nontrivial (anti-)holomorphic solutions to the continuum Euler-Lagrange equation [EL]<sup>cont.</sup>(40) = 0, respectively. These (anti-)holomorphic functions  $f(z) = Cz^{\pm 1} (C\bar{z}^{\pm 1})$  describe the simplest nontrivial (anti-)1-instanton solutions in the continuum  $\mathbb{R}^2$ ; see Appendix A for more details.

#### 3.3. Discrete area evaluated by the zeroth-order solutions

We here evaluate the discrete area (22) using the zeroth-order solutions  $f(z) = Cz^{\pm 1}$  and  $f(z) = C\bar{z}^{\pm 1}$ , obtained in the preceding subsection, in the continuum limit  $\alpha = \pi/M \to +0$  and  $\kappa = q^{-1} - q \to +0$  with fixed discrete conformal structure  $\rho_0 = 2\sin\alpha/\kappa$  (43). Note that the discrete area (22) can also be used with regard to the polar lattice.

A straightforward calculation shows

$$\mathcal{A}(Cz^{\pm 1})_{(M,q)}^{\text{disc.}} = -\mathcal{A}(C\bar{z}^{\pm 1})_{(M,q)}^{\text{disc.}}$$
(65)

$$= |C|^2 M \sin \frac{\pi}{M} \cdot (q^{-1} - q) \sum_{n \in \mathbb{Z}} I_n(|C|, q) q^{2n}, \tag{66}$$

where  $I_n(|C|,q)$  is defined by

$$I_n(|C|,q) := \left(\frac{1}{1 + |C|^2 q^{2n+2}} + \frac{1}{1 + |C|^2 q^{2n-2}}\right)^2 + \left(\frac{2}{1 + |C|^2 q^{2n}}\right)^2. \tag{67}$$

Note that both functions  $f(z) = Cz^{\pm 1}$  give the same expression (66) because of the identity

$$\sum_{n \in \mathbb{Z}} I_n(|C|, q) q^{2n} = \sum_{n \in \mathbb{Z}} I_n(|C|, q^{-1}) q^{-2n}.$$
(68)

Moreover, the factor  $M \sin(\pi/M)$  in (66) is not independent of the other factors because the positive integer M and the common ratio q are related to each other through the fixed discrete conformal structure  $\rho_0$  (43).

After the shifts  $n \to n \pm 1$  in the infinite sum (66), we obtain

$$\mathcal{A}(Cz^{\pm 1})_{(M,q)}^{\mathrm{disc.}} = M\sin\frac{\pi}{M} \cdot \left(\frac{4q}{1+q^2} + |C|^2(q^{-2}+q^2+4)(q^{-1}-q)\sum_{x \in \mathbb{Z}} \frac{q^{2n}}{(1+|C|^2q^{2n})^2}\right). (69)$$

This infinite sum can be written as the q-integral (Jackson integral) [20], and after the limit  $q \to 1-0$  we have

$$(1-q)\sum_{n\in\mathbb{Z}}\frac{q^{2n}}{(1+|C|^2q^{2n})^2} = \int_0^\infty \frac{r}{(1+|C|^2r^2)^2}d_qr \to \int_0^\infty \frac{r}{(1+|C|^2r^2)^2}dr = \frac{1}{2|C|^2}. (70)$$

Note that the  $q^n$  in the infinite sum corresponds to the variable r of the q-integration, i.e.,  $q^n = r$ . Moreover, the range  $0 < r < \infty$  of the q-integration is determined from range  $-\infty < n < \infty$  of the infinite sum.

In the continuum limit where  $\alpha = \pi/M \to +0$  and  $q \to 1-0$  with fixed discrete conformal structure (43), the area (69) tends to the limit  $\pi \cdot (2+6) = 2 \cdot 4\pi$  as expected, because the zeroth-order solutions  $f(z) = Cz^{\pm 1}$  to the discrete Euler–Lagrange equation (56) tend to the corresponding exact solutions in the continuum limit. The extra factor 2 arises for the same reason given in Section 2. For anti-instantons  $f(z) = C\bar{z}^{\pm 1}$ , the area needs an extra minus sign appearing in relation (65).

#### 4. Conclusion and remarks

We have studied a discrete version of the two-dimensional nonlinear O(3) sigma model, which is derived from discrete complex analysis. We adopted two lattices, one rectangular and the other polar. In the rectangular lattice (Section 2), the discrete energy (21) and the area (22) are defined and an inequality (20) that relates the two was derived. In the continuum limit, the discrete energy and area were shown to tend to the usual energy E(f) and area  $\mathcal{A}(f) = 4\pi N$  of the nonlinear O(3) sigma model, up to a factor 2. We have given an explanation for this factor; specifically, the double graph  $\Lambda = \Gamma \cup \Gamma^*$  tends to  $2\mathbb{R}^2$  in the continuum limit giving the factor 2 in the integrations over  $2\mathbb{R}^2$ . We introduced the polar lattice (Section 3), and by imposing a rotationally symmetric ansätze (55), the Euler-Lagrange equation derived from the discrete energy has been reduced to a one-dimensional radial difference equation (56). We obtained the (anti-)holomorphic solutions  $f(z) = Cz^{\pm 1}$  ( $C\bar{z}^{\pm 1}$ ) to the difference equation in the zeroth order of  $\kappa = q^{-1} - q$ . The discrete area (69) evaluated using functions  $f(z) = Cz^{\pm 1}$ can be expressed as the q-integral (Jackson integral), which tends to the expected value  $2 \cdot 4\pi$  in the continuum limit where  $\alpha \to +0$ ,  $q \to 1-0$  and the discrete conformal structure  $\rho_0$  (43) is fixed.

The inequality (20) is saturated if and only if the function f is discrete (anti)holomorphic. Because the area (22) is not a priori a topological invariant, our discrete
energy (21), even though it fulfils the inequality (20), does not ensure topological
stability of the solutions to the Euler-Lagrange equation derived from the discrete
energy. Under certain general assumptions, it was argued in [11] that the energy of
any configuration in the nonlinear O(3) sigma model with nonzero winding number
of [6] is strictly greater than that of the Bogomol'nyi bound. If the discrete area  $|\mathcal{A}(f)^{\text{disc.}}|$  tends to  $2 \cdot 4\pi N$  from above for general f, then we have an inequality  $E(f)^{\text{disc.}} \geq |\mathcal{A}(f)^{\text{disc.}}| > 2 \cdot 4\pi N$  that accords with the argument of [11] except for
the factor 2. A further study is needed on this issue.

There are some interesting open problems remaining. Mercat defined a discrete exponential  $\exp(:\lambda:z) := \prod_k \left(1 + \frac{\lambda\delta}{2}e^{i\theta_k}\right) \left(1 - \frac{\lambda\delta}{2}e^{i\theta_k}\right)^{-1}$  for the vertices  $z = \sum_k \delta e^{i\theta_k}$  with  $\delta$  the lattice spacing of rhombi [13, 14]. This function is discrete holomorphic and tends to the ordinary exponential function  $e^{\lambda x}$  if it is restricted to the real axis  $(\theta_k = 0 \text{ or } \pi)$  and if a continuum limit  $\delta \to 0$  is imposed. If we can define q-exponentials [20] on the polar lattice, then the relationship between these two exponentials is an intriguing problem. Furthermore, although the discrete area (22) is definitively defined algebraically, its geometrical meaning is unclear and we have no exact nontrivial solutions to the difference equation (56) for generic value of q. More detailed research is required on these issues.

#### Acknowledgments

The authors thank T. Sano for helpful discussions about two-dimensional graphs.

#### **Funding**

The Grant-in-Aid for Young Scientists (B) (Grant 25800053) from the Ministry of Education, Culture, Sports, Science and Technology in Japan to Y. T.

# Appendix A. Some continuum instanton solutions

Here we briefly illustrate some continuum (anti-)instanton solutions. The simplest linear function f(z) = z, for example, gives the following instanton solution

$$\mathbf{n} = \left(\frac{2r\cos\theta}{1+r^2}, \frac{2r\sin\theta}{1+r^2}, \frac{1-r^2}{1+r^2}\right),\tag{A.1}$$

where  $(r,\theta)$  are the polar coordinates on  $\mathbb{R}^2$ . This yields  $\lambda(z) = 1/(1+r^2)$  and  $n^3(z) = (1-r^2)/(1+r^2)$ . When r=1, we have  $\boldsymbol{n}=(\cos\theta,\sin\theta,0)$  and the vector  $\boldsymbol{n}$  rotates once when the point (x,y) goes around the circle r=1 once. We have immediately  $n^3(r=0)=1$  and  $\lim_{r\to\infty}n^3(z)=-1$ . Furthermore, the vector  $\boldsymbol{n}$  points to the north pole of the sphere  $S^2_{|\boldsymbol{n}|=1}$  at the origin and points to the south pole at infinity. This suggests that the vector (A.1) is an N=1 instanton solution; indeed, we can verify this as  $N=(4\pi)^{-1}\int_{\mathbb{R}^2}d^2x\,4(1+r^2)^{-2}=1$ .

Next, the simplest quadratic function  $f(z) = z^2$  yields

$$\boldsymbol{n} = \left(\frac{2r^2\cos 2\theta}{1+r^4}, \frac{2r^2\sin 2\theta}{1+r^4}, \frac{1-r^4}{1+r^4}\right). \tag{A.2}$$

Here we have  $\lambda(z)=1/(1+r^4)$  and  $n^3(z)=(1-r^4)/(1+r^4)$ . As  $r\to\infty$ ,  $\lambda(z)$  decreases more rapidly than that for the linear function. When r=1, we have  $\boldsymbol{n}=(\cos 2\theta,\sin 2\theta,0)$  and the vector  $\boldsymbol{n}$  rotates twice when the point (x,y) goes around the circle r=1 once. The vector (A.2) is actually an N=2 instanton solution as verified by  $N=(4\pi)^{-1}\int_{\mathbb{R}^2}d^2x\,4r^4(1+r^4)^{-2}=2$ .

The vector  $\boldsymbol{n}$  derived from the function  $f(z)=z^{-1}$ , which has a pole at z=0, is given by

$$\boldsymbol{n} = \left(\frac{2r^{-1}\cos\theta}{1+r^{-2}}, -\frac{2r^{-1}\sin\theta}{1+r^{-2}}, \frac{1-r^{-2}}{1+r^{-2}}\right) = \left(\frac{2r\cos\theta}{1+r^2}, -\frac{2r\sin\theta}{1+r^2}, -\frac{1-r^2}{1+r^2}\right). \tag{A.3}$$

Note that (A.3) is obtained from (A.1) by replacing variables  $(r,\theta)$  by  $(1/r,-\theta)$ . Although the function  $f(z)=z^{-1}$  has a pole at the origin, the last expression in (A.3) does not have any singularities at r=0; the singularities of the vector  $\mathbf{n}$  at r=0 are "removable". As the second and third components of (A.3) have extra minus signs compared with (A.1), and the scalar triple product  $\mathbf{n} \cdot (\partial_x \mathbf{n} \times \partial_y \mathbf{n})$  is invariant under a change of sign of the two components of the vector  $\mathbf{n}$ , we have N=1 for (A.3). Because we have  $\lambda(z) = r^2/(1+r^2)$  and  $n^3(z) = -(1-r^2)/(1+r^2)$  from (A.3) as well as  $n^3(r=0) = -1$  and  $\lim_{r\to\infty} n^3(z) = 1$ , the vector (A.3) is an N=1 instanton solution with boundary conditions opposite to those of (A.1).

As for the anti-instantons, their vectors  $\mathbf{n}$  are obtained from (A.1-A.3) of the instantons by mapping angle  $\theta \to -\theta$ , resulting in a change in sign of their second

components. Because the scalar triple product  $\mathbf{n} \cdot (\partial_x \mathbf{n} \times \partial_y \mathbf{n})$  changes sign by changing the sign of one component of the vector  $\mathbf{n}$ , the topological number N of an anti-instanton is given by the instanton of opposite sign.

# Appendix B. Expansion of functions in the parameter $\kappa$

We derive several expansion formulae used in Section 3.2. We begin with the function y of  $\kappa = q^{-1} - q$  (0 < q < 1)

$$y(\kappa) := \varphi(q^{\pm 1}r), \tag{B.1}$$

where  $\varphi(r)$  is an arbitrary differentiable function of the radius r, which we consider as a parameter. Explicit forms of  $q^{\pm 1}$  as functions of  $\kappa$  are given by

$$q^{\pm 1} = \sqrt{1 + \frac{\kappa^2}{4}} \mp \frac{\kappa}{2}.\tag{B.2}$$

Because the limit  $\kappa \to +0$  is equivalent to the limit  $q \to 1-0$ , we have  $y(0) = \varphi(r)$ . The first and second derivatives of  $y(\kappa)$  with respect to  $\kappa$  are given by

$$y'(\kappa) = r\varphi'(q^{\pm 1}r)\frac{dq^{\pm 1}}{d\kappa}, \quad y''(\kappa) = r^2\varphi''(q^{\pm 1}r)\left(\frac{dq^{\pm 1}}{d\kappa}\right)^2 + r\varphi'(q^{\pm 1}r)\frac{d^2q^{\pm 1}}{d\kappa^2},$$
 (B.3)

from which we have

$$y'(0) = \mp r\varphi'(r), \ y''(0) = \frac{1}{4}(r^2\varphi''(r) + r\varphi'(r)),$$
 (B.4)

where we have used

$$\frac{dq}{d\kappa} = -\frac{q^2}{1+q^2}, \qquad \frac{dq^{-1}}{d\kappa} = \frac{1}{1+q^2}, \qquad \frac{d^2q}{d\kappa^2} = \frac{d^2q^{-1}}{d\kappa^2} = \frac{2q^3}{(1+q^2)^3}.$$
 (B.5)

A similar procedure gives the third derivative

$$y'''(0) = \mp \frac{1}{4} (r^3 \varphi'''(r) + 3r^2 \varphi''(r)). \tag{B.6}$$

Hence we obtain the expansion formula

$$\varphi(q^{\pm 1}r) = \varphi \mp \frac{1}{2}r\varphi'\kappa + \frac{1}{8}\left(r^2\varphi'' + r\varphi'\right)\kappa^2 \mp \frac{1}{48}\left(r^3\varphi''' + 3r^2\varphi''\right)\kappa^3 + o(\kappa^3), \quad (B.7)$$

where the argument of  $\varphi$  on the right-hand side is r. Analogously, we obtain an expansion formula for  $\varphi(q^{\pm 2}r)$ 

$$\varphi(q^{\pm 2}r) = \varphi \mp r\varphi'\kappa + \frac{1}{2}\left(r^2\varphi'' + r\varphi'\right)\kappa^2 \mp \frac{1}{24}\left(4r^3\varphi''' + 12r^2\varphi' + 3r\varphi'\right)\kappa^3 + o(\kappa^3).$$
(B.8)

The second-order differential equation (59) for h(r) is obtained by employing the expansion formulae (B.7) and (B.8).

#### REFERENCES

- [1] BELAVIN, A. A., POLYAKOV, A. M., SCHWARZ, A. S. & TYUPKIN, Yu. S. (1975) Pseudoparticle solutions of the Yang-Mills equations. *Phys. Lett. B.*, **59**, 85-87.
- [2] BOGOMOL'NYI, E. B. (1976) The stability of classical solutions. Sov. J. Nucl. Phys., 24, 449-454; PRASAD, M. K. & SOMMERFIELD, C. M. (1975) Exact Classical Solution for the 't Hooft Monopole and the Julia-Zee Dyon. Phys. Rev. Lett., 35, 760-762.
- [3] BELAVIN, A. A. & POLYAKOV, A. M. (1975) Metastable states of two-dimensional isotropic ferromagnets. Sov. Phys.-JETP Lett., 22, 245-248, Pisma Zh. Eksp. Teor. Fiz., 22, 503-506.
- [4] RAJARAMAN, R. (1987) Solitons and Instantons. North-Holland Personal Library, Amsterdam: North-Holland Physics Publishing.
- [5] MANTON, N. & SUTCLIFFE, P. (2004) *Topological Solitons*. Cambridge Monographs on Mathematical Physics, Cambridge: Cambridge Univ. Press.
- [6] BERG, B. & LÜSCHER, M. (1981) Definition and statistical distributions of a topological number in the lattice O(3) σ-model. Nucl. Phys. B., 190, 412-424.
- [7] SPEIGHT, J. M. & WARD, R. S. (1994) Kink dynamics in a novel discrete sine-Gordon system. Nonlinearity, 7, 475-484.
- [8] PIETTE, B. M. A. G., SCHROERS, B. J. & ZAKRZEWSKI, W. J. (1995) Multisolitons in a Twodimensional Skyrme Model. Z. Phys. C., 65, 165-174.
- [9] WARD, R. S. (1995) Stable Topological Skyrmions on the 2D Lattice. Lett. Math. Phys., 35, 385-393.
- [10] LEESE, R. (1989) Discrete Bogomolny equations for the nonlinear O(3)  $\sigma$  model in 2+1 dimensions. Phys. Rev. D., 40, 2004-2013.
- [11] WARD, R. S. (1997) Bogomol'nyi bounds for two-dimensional lattice systems. *Comm. Math. Phys.*, **184**, 397-410.
- [12] WILSON, S. O. (2008) Conformal cochains. Trans. Amer. Math. Soc., 360, 5247-5264.
- [13] MERCAT, C. (2001) Discrete Riemann surfaces and Ising model. Comm. Math. Phys., 218, 177-216.
- [14] MERCAT, C. (2007) Discrete Riemann surfaces. (Handbook of Teichmüller theory. Vol. I, 541–575, IRMA Lect. Math. Theor. Phys., 11, Eur. Math. Soc. Zürich); arXiv:0802.1612v1 [math.CV].
- [15] BOBENKO, A. I. & SURIS, Y. B. (2008) Discrete Differential Geometry: Integrable Structure (Graduate Studies in Mathematics, Vol. 98, AMS)
- [16] BOBENKO, A. I. & GÜNTHER, F. (2017) Discrete Riemann surfaces based on quadrilateral cellular decompositions. Adv. Math., 311, 885-932.
- [17] DUFFIN, R. J. (1956) Basic properties of discrete analytic functions. Duke Math. J., 23, 335-363.
- [18] DUFFIN, R. J. (1968) Potential theory on a rhombic lattice. J. Combinatorial Theory, 5, 258-272.
- [19] ZLÁMAL, M. (1968) On the finite element method. Numer. Math., 12, 394-409.
- [20] GASPER, G. & RAHMAN, M. (2004) Basic Hypergeometric Series, 2nd edn. Encyclopedia of Mathematics and its Applications, Vol. 96. Cambridge: Cambridge Univ. Press.